Supplementary Information

Tuning selectivity of CO_2 hydrogenation by modulating the strong metal–support interaction over Ir/TiO_2 catalysts

Yaru Zhang,[a,b] Zhen Zhang,[c] Xiaofeng Yang,[a] Ruifeng Wang,[a] Hongmin Duan,[a] Zheng Shen,[a] Lin Li,[a] Yang Su,[a] Runze Yang,[c] Yongping Zhang,[c] Xiong Su,*[a] Yanqiang Huang,*[a] and Tao Zhang[d]

[a] CAS Key Laboratory of Science and Technology on Applied Catalysis, Dalian Institute of Chemical Physics, Chinese Academy of Sciences, Dalian 116023, China

[b] University of Chinese Academy of Sciences, Beijing 100049, China

[c] China Astronaut Research and Training Center, Beijing 100094, China

[d] State Key Laboratory of Catalysis, Dalian Institute of Chemical Physics, Chinese Academy of Sciences, Dalian 116023, China

*To whom correspondence should be addressed. E-mail: yqhuang@dicp.ac.cn (Y. Huang) and suxiong@dicp.ac.cn (X. Su).

Supplementary Figures

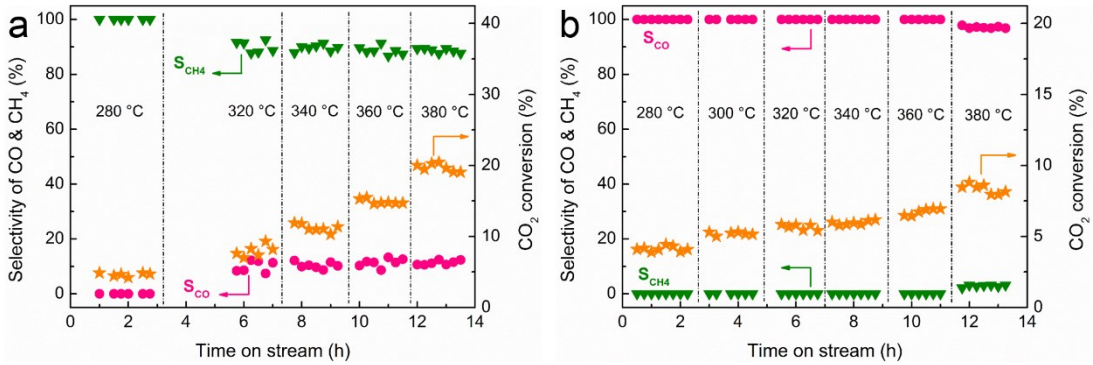

Fig. S1. Evolution of catalytic performance versus time and reaction temperature, over the (a) Ir/TiO_2-200 and (b) Ir/TiO_2-700 catalysts. Reaction conditions: atmospheric pressure, space velocity = 9000 mL h^{-1} $gcat^{-1}$, $H_2/CO_2/N_2$ = 70/20/10.

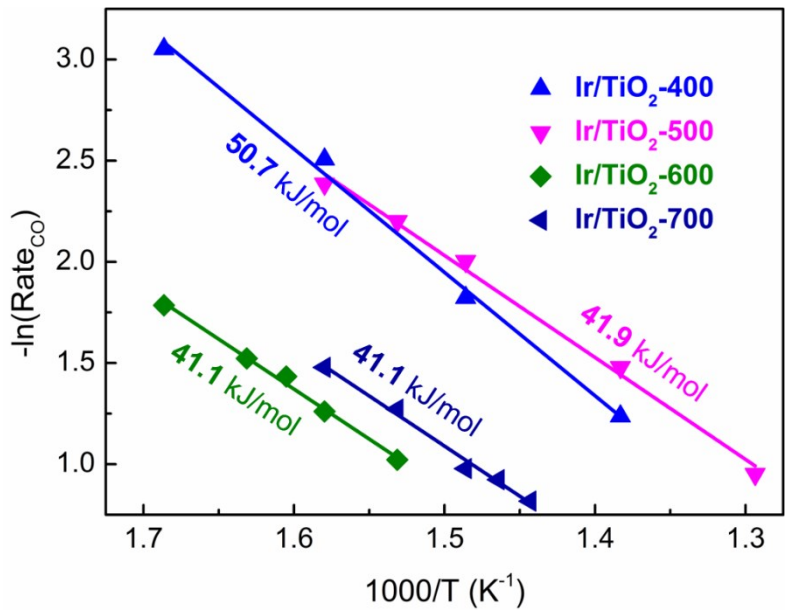

Fig. S2. Arrhenius plots for CO production over the Ir/TiO_2-*x* catalysts.

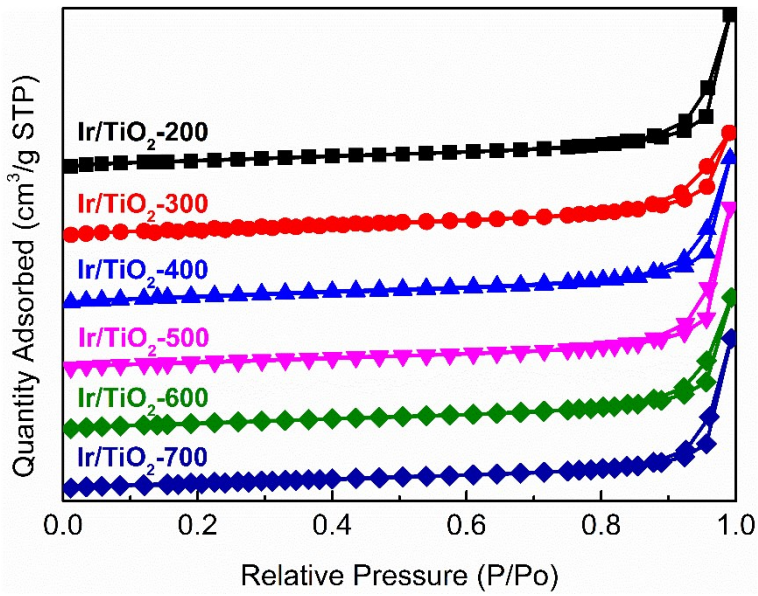

Fig. S3. N_2 adsorption-desorption isotherms for the series Ir/TiO_2-*x* catalysts.

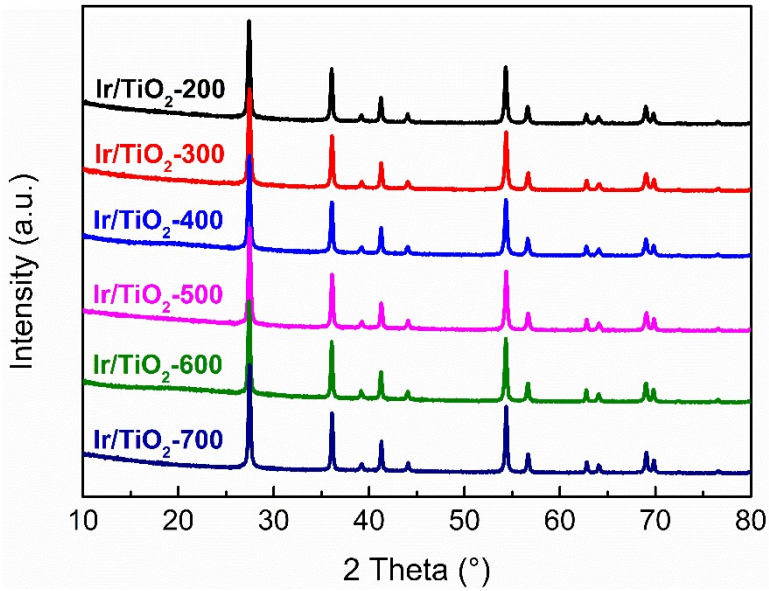

Fig. S4. XRD patterns of the series Ir/TiO_2-*x* catalysts.

Supplementary Tables

Table S1. Comparison of the catalytic performance for CO_2 hydrogenation over different catalysts.

Entry	Catalyst	H_2/CO_2	P (MPa)	T (°C)	Reaction rate ($mol_{CO2}\ g_{metal}^{-1}\ h^{-1}$)	S_{CH4} (%)	S_{CO} (%)	Ref.
1	2.45 wt% Ir/TiO_2-200	3.5	0.1	280	0.159	100	0	This work
2	2.45 wt% Ir/TiO_2-700	3.5	0.1	280	0.146	0	100	
3	2.45 wt% Ir/TiO_2-200	3.5	0.1	400	0.769	87.4	12.6	
4	0.1 wt% Ir_1/TiO_2	1	0.1	350	0.043	0	~100	1
5	0.7 wt% Ir/Ce	4	1.0	300	0.422	trace	> 99	2
6	20 wt% Ir/Ce	4	1.0	300	0.045	88	12	
7	6 wt% Rh/TiO_2	1	0.1	200	0.028	98	2	3
8	2.56 wt% Ru(NC)/CeO_2	4	0.1	190	0.264	> 98	< 2	4
9	5 wt% Ru/r-TiO_2	4	0.1	200	0.73	100	0	5
10	0.5 wt% Pd/Al_2O_3	3	0.1	300	0.128	~10	~90	6
11	0.1 wt% Pt/TiO_2	1	0.1	250	0.024	< 2	> 98	7
12	4 wt% $AuMo/SiO_2$	2	0.81	300	0.525	0	100	8
13	10 wt% Co/r-TiO_2	4	3.0	400	0.549	99.8	0.2	9
14	10 wt% Co/a-TiO_2	4	3.0	400	0.091	10.5	89.5	
15	5 wt% Ni/a-TiO_2	4	0.1	360	0.127	0	100	10
16	5 wt% Ni/a-TiO_2-NH_3	4	0.1	360	1.481	96.9	3.1	

A comparison of the catalytic performance for CO_2 hydrogenation in this work with that of state-of-the-art catalysts as well as catalysts without precious metals is shown in Table S1.

As compared with other reported Ir-based catalysts (Entry 4–6), Ir/TiO_2-200 in this work exhibits a much higher activity for CO_2 methanation, and Ir/TiO_2-700 catalyst exhibits at least comparable activity for reverse water-gas shift reaction.

For Sabatier reaction (Entry 7–9), the activity of Ir/TiO_2-200 in this work is inferior to that of Ru-based catalysts, but at least a comparable value with that of Rh-based catalysts. As for reverse water-gas shift reaction (Entry 10–12), Ir/TiO_2-700 exhibits comparable or higher activity with the reported catalysts.

When it comes to Co-based (Entry 13, 14) or Ni-based (15, 16) catalysts for CO_2 hydrogenation, a higher reaction temperature or pressure is usually employed to initiate CO_2 activation. For CO_2 methanation, the Ir/TiO_2-200 catalyst shows a higher activity than Co-based catalysts, but lower than that of Ni-based catalysts. For reverse water-gas shift reaction, the Ir/TiO_2-700 catalyst shows a higher activity than both Co-based and Ni-based catalysts.

Table S2. Apparent activation energies obtained from Arrhenius plots for the series Ir/TiO_2-*x* catalysts.

Catalyst	E_a (CO_2) (kJ mol^{-1})	E_a (CO) (kJ mol^{-1})	E_a (CH_4) (kJ mol^{-1})
Ir/TiO_2-200	42.5	–	39.6
Ir/TiO_2-300	40.5	–	42.0
Ir/TiO_2-400	45.4	50.7	44.1
Ir/TiO_2-500	40.5	41.9	58.4
Ir/TiO_2-600	44.1	41.1	110.6
Ir/TiO_2-700	47.1	41.1	233.9

Table S3. BET surface areas and pore volumes of the series Ir/TiO_2 catalysts pretreated at different temperatures (Ir/TiO_2-*x* samples).

Catalyst	S_{BET} (m^2 g^{-1})	V_{pore} (cm^3 g^{-1})
Ir/TiO_2-200	26	0.038
Ir/TiO_2-300	27	0.041
Ir/TiO_2-400	26	0.038
Ir/TiO_2-500	25	0.036
Ir/TiO_2-600	25	0.037
Ir/TiO_2-700	25	0.033

Table S4. The crystal parameters of rutile-type IrO_2 and TiO_2.

Oxide	Crystal form	M–O bond distance (nm)	Lattice spacing (nm)	
			a, b axis	c axis
IrO_2	rutile	0.1958	0.4505	0.3158
TiO_2	rutile	0.1980	0.4594	0.2958

Table S5. H_2 consumption results of the Ir/TiO_2 catalyst.

Sample	H_T, theoretical value[a] (μmol g^{-1})	H_M, measured value by H_2-TPR (μmol g^{-1})			H_M/H_T
		50–285 °C	285–800 °C	50–800 °C	
Ir/TiO_2	254.9	253.7	149.0	402.7	1.6

[a] The theoretical H_2 consumption (H_T) was estimated by the assumption of complete IrO_2 reduction with 2.45 wt% Ir loading.

Table S6. Quantified XPS data for surface Ti on the series Ir/TiO_2-*x* catalysts.

Sample	Ti^{4+}			Ti^{3+}		
	Bind energy (eV)		Content	Bind energy (eV)		Content
	$2p_{1/2}$	$2p_{3/2}$		$2p_{1/2}$	$2p_{3/2}$	
Ir/TiO_2-200	464.1	458.5	98.9%	463.3	457.8	1.1%
Ir/TiO_2-400	464.1	458.5	92.7%	463.2	457.7	7.3%
Ir/TiO_2-600	464.1	458.4	91.4%	463.2	457.7	8.6%
Ir/TiO_2-700	464.1	458.4	90.3%	463.2	457.7	9.7%

References

1. X. Chen, X. Su, H.-Y. Su, X. Liu, S. Miao, Y. Zhao, K. Sun, Y. Huang and T. Zhang, *ACS Catal.*, 2017, **7**, 4613–4620.
2. S. Li, Y. Xu, Y. Chen, W. Li, L. Lin, M. Li, Y. Deng, X. Wang, B. Ge, C. Yang, S. Yao, J. Xie, Y. Li, X. Liu and D. Ma, *Angew. Chem. Int. Ed.*, 2017, **56**, 10761–10765.
3. J. C. Matsubu, S. Zhang, L. DeRita, N. S. Marinkovic, J. G. Chen, G. W. Graham, X. Pan and P. Christopher, *Nat. Chem.*, 2016, **9**, 120–127.
4. Y. Guo, S. Mei, K. Yuan, D.-J. Wang, H.-C. Liu, C.-H. Yan and Y.-W. Zhang, *ACS Catal.*, 2018, **8**, 6203–6215.
5. J. Xu, X. Su, H. Duan, B. Hou, Q. Lin, X. Liu, X. Pan, G. Pei, H. Geng, Y. Huang and T. Zhang, *J. Catal.*, 2016, **333**, 227–237.
6. J. H. Kwak, L. Kovarik and J. Szanyi, *ACS Catal.*, 2013, **3**, 2094–2100.
7. X. Chen, X. Su, H. Duan, B. Liang, Y. Huang and T. Zhang, *Catal. Today*, 2017, **281**, 312–318.
8. R. Carrasquillo-Flores, I. Ro, M. D. Kumbhalkar, S. Burt, C. A. Carrero, A. C. Alba-Rubio, J. T. Miller, I. Hermans, G. W. Huber and J. A. Dumesic, *J. Am. Chem. Soc.*, 2015, **137**, 10317–10325.
9. W. Li, G. Zhang, X. Jiang, Y. Liu, J. Zhu, F. Ding, Z. Liu, X. Guo and C. Song, *ACS Catal.*, 2019, **9**, 2739–2751.
10. J. Li, Y. Lin, X. Pan, D. Miao, D. Ding, Y. Cui, J. Dong and X. Bao, *ACS Catal.*, 2019, **9**, 6342–6348.